

Island-based Random Dynamic Voltage Scaling vs ML-Enhanced Power Side-Channel Attacks

Dake Chen
University of Southern California
Los Angeles, California, USA
dakechen@usc.edu

Christine Goins
Niobium Microsystems, Inc.
Dayton, Ohio, USA
christine@niobiummicrosystems.com

Maxwell Waugaman
Independent Researcher
Washington, USA
wellwaugaman@gmail.com

Georgios D. Dimou
Niobium Microsystems, Inc.
Dayton, Ohio, USA
georgios@niobiummicrosystems.com

Peter A. Beerel
University of Southern California
Los Angeles, California, USA
pabeerel@usc.edu

ABSTRACT

In this paper, we describe and analyze an island-based random dynamic voltage scaling (iRDVS) approach to thwart power side-channel attacks. We first analyze the impact of the number of independent voltage islands on the resulting signal-to-noise ratio and trace misalignment. As part of our analysis of misalignment, we propose a novel unsupervised machine learning (ML) based attack that is effective on systems with three or fewer independent voltages. Our results show that iRDVS with four voltage islands, however, cannot be broken with 200k encryption traces, suggesting that iRDVS can be effective. We finish the talk by describing an iRDVS test chip in a 12nm FinFet process that incorporates three variants of an AES-256 accelerator, all originating from the same RTL. This included a synchronous core, an asynchronous core with no protection, and a core employing the iRDVS technique using asynchronous logic. Lab measurements from the chips indicated that both unprotected variants failed the test vector leakage assessment (TVLA) security metric test, while the iRDVS was proven secure in a variety of configurations.

CCS CONCEPTS

• **Security and privacy** → **Side-channel analysis and countermeasures**; • **Computing methodologies** → **Unsupervised learning**.

KEYWORDS

Hardware security; Side-channel attack; Machine learning

ACM Reference Format:

Dake Chen, Christine Goins, Maxwell Waugaman, Georgios D. Dimou, and Peter A. Beerel. 2023. Island-based Random Dynamic Voltage Scaling vs ML-Enhanced Power Side-Channel Attacks. In *Proceedings of the Great Lakes Symposium on VLSI 2023 (GLSVLSI '23)*, June 5–7, 2023, Knoxville, TN, USA. ACM, New York, NY, USA, 7 pages. <https://doi.org/10.1145/3583781.3590266>

Permission to make digital or hard copies of part or all of this work for personal or classroom use is granted without fee provided that copies are not made or distributed for profit or commercial advantage and that copies bear this notice and the full citation on the first page. Copyrights for third-party components of this work must be honored. For all other uses, contact the owner/author(s).
GLSVLSI '23, June 5–7, 2023, Knoxville, TN, USA
© 2023 Copyright held by the owner/author(s).
ACM ISBN 979-8-4007-0125-2/23/06.
<https://doi.org/10.1145/3583781.3590266>

1 INTRODUCTION

With billions of computing devices being deployed in the Internet of Things, autonomous vehicles and other pervasive applications, ensuring our integrated circuits are secure has become as important as improving performance, power, and area. In particular, power side-channel attacks have become an increasing source of concern [11].

Various countermeasures against power side-channel attacks have been proposed, including masking to make power signatures independent from cryptographic keys [8], current flattening using sophisticated power delivery mechanisms [10], and increasing the difficulty of trace alignment, a critical step in power attacks [9, 13]. Alignment techniques have co-evolved with these countermeasures. Powerful approaches for aligning traces include “time warping” techniques, such as elastic alignment [21] and the rapid alignment method [2]. The countermeasure closest to that proposed in this paper is *dynamic voltage scaling* (DVS). DVS affects both the timing and amplitude of power traces [1, 20, 23]. However, most DVS approaches have been restricted to using a single voltage for the entire design and are vulnerable to the estimation of the random voltage [1]. Machine learning techniques have been extensively used for attacking hardware security systems [7]. In particular, with the help of the unsupervised machine learning algorithm, we show that DVS can be effectively attacked by grouping the power traces into clusters with similar supply voltages and attacking one cluster.

This paper proposes and analyzes an *island-based random dynamic voltage scaling* (iRDVS) approach that uses multiple independent random voltages that are more difficult to estimate. We first analyze the *signal-to-noise ratio* (SNR) of iRDVS, then analyze the resistance of this technique to alignment. We evaluate both as a function of the number of independent voltages. Together, we argue, these analyses suggest that a design with a small number of independent voltages achieves high security.

As part of our alignment analysis, we propose a novel applied unsupervised ML algorithm to cluster iRDVS traces and enable more effective power attacks. Our approach, uses clustering to classify power traces from different unknown iRDVS voltages into groups of similar voltages. Our experimental results show that this clustering-based attack is able to uncover keys in systems protected by one, two and three dynamic voltage islands but has limited benefit when applied to iRDVS schemes with four or more islands.

The rest of the paper is organized as follows. Section 2 describes the techniques and metrics used in this paper. Section 3 proposes

the iRDVS design. Section 4 and Section 5 analyze the SNR and misalignment characteristics of our approach as a function of the number of islands, and Section 6 focuses on our proposed ML attack. Section 7 and Section 8 describes the details of our simulation experiments and measurement results. Finally, we provide a summary of this work with our plans for future work in Section 9.

2 BACKGROUND

This section summarizes correlation-based power analysis, provides details on the elastic alignment technique used to test our approach, and introduces three common metrics for quantifying countermeasure effectiveness.

2.1 Correlation-Based Power Analysis

Power analysis attacks take advantage of the dependence of a circuit's power consumption on the data it processes. A common method of disclosing this correlation employs a differential technique introduced by Kocher et al. [11] called *differential power analysis (DPA)* that recovers keys bit-by-bit. Another powerful technique requiring less knowledge of the algorithm implementation, introduced by Brier et al., is *correlation-based power analysis (CPA)* [5]. Brier et al. demonstrated that all countermeasures against CPA provide similar defensive effectiveness against DPA. Moreover, CPA is capable of attacking several bits at a time instead of only a single bit. Because of this advantage, we applied CPA in our experiments.

2.2 Elastic Alignment

Woudenberg et al. [21] propose a powerful alignment algorithm, *elastic alignment*, to preprocess traces corrupted by random delay insertion or an unstable clock. The two step procedure aligns recorded traces to a single reference. First, it leverages a traditional algorithm, *dynamic time warping*, to find a *warp path* that maps the time steps of each sample trace to those of a reference trace. To do this, the algorithm computes the Euclidean difference between each target trace t and a reference trace r , captured in a 2-D cost matrix of size $P \times Q$, where P and Q are the lengths of traces t and r , respectively. It then applies dynamic programming to identify the minimum-cost path through the matrix between points $(0, 0)$ and (P, Q) . This path defines the correspondence between traces r and t . Secondly, guided by this path, elastic alignment averages across samples when multiple samples of t map to one time step and duplicates samples of t when one sample of t maps to multiple time steps. We reproduce this approach and show it can effectively align the traces corrupted by the frequency-scaled technique.

2.3 Metrics for Countermeasure Effectiveness

There are three common metrics for measuring side-channel countermeasure effectiveness. The first is *Minimum Traces to Disclosure (MTD)*, which is the number of encryption/decryption traces required to disclose all of the secret information. A higher MTD indicates a more secure countermeasure. This metric requires that all bytes of the secret are guessed correctly. *Partial Guessing Entropy (PGE)* [17] can be a more practical evaluation metric than MTD because it does not require a correctly-guessed secret. PGE is computed from the ranking of possible values of the subkey bytes in

descending order of correlation as estimated by the Pearson correlation coefficient. PGE is the rank of the correct subkey, where a PGE of 0 denotes that the subkey was correctly guessed. A large PGE indicates a low correlation of the correct subkey and consequently a system robust to attacks. The *Test Vector Leakage Analysis (TVLA)* is also commonly used to evaluate side-channel leakage [3]. The test conducts two experiments with fixed and random plaintexts and generates a large number of traces respectively, and the power samples from two groups are used for calculating a t-score at each time step. The t-score is a statistical measure of how different traces from the fixed and random encryptions are from one another. A higher t-score indicates that the difference between the fixed and random traces is less likely to have occurred by chance, suggesting the device exhibits higher leakage that would make a power analysis attack more likely to succeed.

3 ISLAND-BASED RANDOM DVS

Traditional DVS countermeasures can be attacked if the random dynamic voltage is uncovered [1]. Attackers can scale measured power traces in time and amplitude to match a reference trace, which renders DVS designs vulnerable.

To circumvent the weaknesses of single-island DVS, this paper proposes using several independent voltages in an *island-based random DVS (iRDVS)* framework, illustrated in Figure 1. iRDVS makes side-channel attacks more difficult because attackers must differentiate between multiple simultaneous random dynamic voltages.

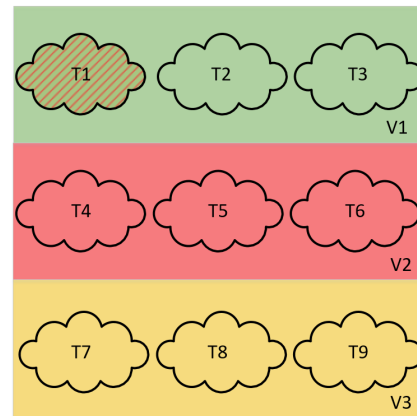


Figure 1: Illustration of a typical iRDVS structure with $n = 9$ islands and $m = 3$ independent voltages. Each independent voltage domain has a different color and each cloud represents a group of logic; the shaded logic is under attack.

One practical means of implementing this iRDVS framework for a pipelined design is to partition each combinational stage into multiple islands with independent voltages. The voltages can be randomly adjusted with the constraint that the delay of each pipeline stage is roughly the same, thereby maximizing overlapping computation and minimizing the chance of introducing timing side channels. Multiple islands can share one voltage supply to support scaling this approach to large circuits with many islands. The islands need not all be the same size but can be adjusted based on both logical and physical constraints and communicate using asynchronous channels that implement the flow-control necessary to

cope with different stage delays [4] We assume each island will have an on-chip DC/DC converter whose control will leverage the entropy from an off-the-shelf true random number generator (TRNG). This is similar to the random voltage generation proposed for random DVS [12, 22, 24]. As was implemented in [12], we assume the TRNGs will be on-die and thus not directly accessible to power attacks. Determining the optimal number and configuration of independent voltages that not only thwarts voltage prediction but also retains the statistical merits of DVS is one of the key research objectives we explore here.

4 SNR ANALYSIS

The *signal-to-noise ratio* (SNR) is typically used to quantify how well the secret portion of the computation is hidden within the overall power consumption [16]. The SNR is defined as $SNR = \frac{Var(AP)}{Var(N)}$ where AP denotes the power consumption associated with the intermediate value that carries secret information and N consists of the power consumption of uncorrelated computations and electronic noise. In this section, we examine the SNR of various island configurations to analyze their effectiveness. To simplify our analysis, we assume the traces are perfectly aligned; we analyze the misalignment benefit associated with iRDVS in the next section.

The correlation between the hypothetical intermediate value and power traces can be derived in terms of SNR:

$$\rho = \frac{\rho_{ap}}{\sqrt{1 + \frac{1}{SNR}}} \quad (1)$$

where ρ_{ap} denotes the correlation between the power consumption of the attacked part and the hypothetical intermediate value [16]. This equation shows that a lower SNR leads to a lower correlation, which indicates higher robustness.

Let T_i be a power trace for island i normalized by the voltage of that island. Let v_i denote the independent random dynamic supply voltage for island i . Because the switching power is proportional to v^α , where $\alpha \approx 2$, and most instantaneous power consumption is from switching power, the DVS power traces are proportional to $v^\alpha T$. Let n denote the number of independent islands and m represent the number of independent voltages used. We present three different cases for comparison: first, the $m = n$ independent DVS case, which means we assign a different random voltage to each island; then, the cases with two ($m = 2$) and one ($m = 1$) independent voltages.

Without loss of generality, assume the first island is attacked, so the power consumption of the other $n - 1$ islands is switching noise. The SNR for $m = n$ iRDVS islands (v_1, v_1, \dots, v_n) can be represented as follows. Let σ and μ denote the standard deviation and mean of their associated variables, respectively. Since v_i and T_i are independent of each other, we can expand the variance for both denominator and numerator.

$$SNR_{m=n} = \frac{Var(v_1^\alpha T_1)}{Var(\sum_{i=2}^n v_i^\alpha T_i)} \quad (2)$$

$$= \frac{\sigma_{v_1^\alpha}^2 \sigma_{T_1}^2 + \sigma_{v_1^\alpha}^2 \mu_{T_1}^2 + \mu_{v_1^\alpha}^2 \sigma_{T_1}^2}{\sum_{i=2}^n (\sigma_{v_i^\alpha}^2 \sigma_{T_i}^2 + \sigma_{v_i^\alpha}^2 \mu_{T_i}^2 + \mu_{v_i^\alpha}^2 \sigma_{T_i}^2)} \quad (3)$$

Considering the special case that variances and means of the island power consumption and supply voltages are the same, denoted σ_T^2 , μ_T , $\sigma_{v^\alpha}^2$ and μ_{v^α} , we obtain:

$$SNR_{m=n} = \frac{\sigma_{v^\alpha}^2 \sigma_T^2 + \sigma_{v^\alpha}^2 \mu_T^2 + \mu_{v^\alpha}^2 \sigma_T^2}{(n-1)\sigma_{v^\alpha}^2 \mu_T^2 + (n-1)(\mu_{v^\alpha}^2 \sigma_T^2 + \sigma_{v^\alpha}^2 \sigma_T^2)} \quad (4)$$

Similarly, we can derive the SNR for the cases where m is equal to two (v_1, v_2) and one (v) independent voltages, the latter modeling the conventional DVS approach.

$$SNR_{m=2} = \frac{Var(v_1^\alpha T_1)}{Var(v_1^\alpha \sum_{i=2}^{\frac{n}{2}} T_i + v_2^\alpha \sum_{i=\frac{n}{2}+1}^n T_i)} \\ = \frac{\sigma_{v_1^\alpha}^2 \sigma_{T_1}^2 + \sigma_{v_1^\alpha}^2 \mu_{T_1}^2 + \mu_{v_1^\alpha}^2 \sigma_{T_1}^2}{[(\frac{n}{2}-1)^2 + (\frac{n}{2})^2] \sigma_{v_1^\alpha}^2 \mu_{T_1}^2 + (n-1)(\sigma_{v_1^\alpha}^2 \sigma_{T_1}^2 + \mu_{v_1^\alpha}^2 \sigma_{T_1}^2)} \quad (5)$$

$$SNR_{m=1} = \frac{Var(v_1^\alpha T_1)}{Var(v_1^\alpha \sum_{i=2}^n T_i)} \\ = \frac{\sigma_{v_1^\alpha}^2 \sigma_T^2 + \sigma_{v_1^\alpha}^2 \mu_T^2 + \mu_{v_1^\alpha}^2 \sigma_T^2}{(n-1)^2 \sigma_{v_1^\alpha}^2 \mu_T^2 + (n-1)(\sigma_{v_1^\alpha}^2 \sigma_T^2 + \mu_{v_1^\alpha}^2 \sigma_T^2)} \quad (6)$$

Due to the algebraic property that for $a \geq 1$ and $b \geq 1$, $(a+b)^2 \geq a^2 + b^2 \geq a + b$, it can easily be shown that $SNR_{m=n} \geq SNR_{m=2} \geq SNR_{m=1}$. This indicates that, somewhat counter-intuitively, without considering the misalignment and temporal advantage, a lower number of DVS islands results in lower SNR, thereby lower correlation and higher robustness.

We can explain this trend more generally from the perspective of covariance:

$$Var(v_i^\alpha T_i + v_j^\alpha T_j) = Var(v_i^\alpha T_i) + Var(v_j^\alpha T_j) + 2Cov(v_i^\alpha T_i, v_j^\alpha T_j) \quad (7)$$

The above equation is the general formula for computing the variance of two islands. If the two islands have the same supply voltage, i.e., $v_i = v_j$, the two quantities $v_i^\alpha T_i$ and $v_j^\alpha T_j$ are correlated, therefore the covariance term $Cov(v_i^\alpha T_i, v_j^\alpha T_j)$ is greater than zero. When the two islands have independent random voltages with possibly different means and variances, i.e., $v_i \neq v_j$ where σ_T^2 , μ_T , $\sigma_{v^\alpha}^2$ and μ_{v^α} are not equal, the two quantities $v_i^\alpha T_i$ and $v_j^\alpha T_j$ are also independent and $Cov(v_i^\alpha T_i, v_j^\alpha T_j) = 0$.

This reduction in variance caused by an increasing number of supply voltages can be generalized to more islands. For the case of $m = 2$, the $\frac{n}{2}$ noise islands supplied by v_2 are correlated with one another, increasing the covariance terms in the denominator and decreasing the SNR. However, if we keep n constant and increase the number of voltage supplies m , the correlation between islands reduces (increasing SNR) because fewer islands are correlated with each other. When $m = n$, each island is powered by an independent supply so there is no covariance among noise islands. Therefore, the variance of the noise is minimized and the SNR is maximized for this n .

We experimentally verified this trend by performing CPA on a simplified model of AES that simulated the Sbox operations in the first round of AES. This model, given a plaintext, computes the 16 Sbox output values for the first round of AES and generates a power pulse with a peak amplitude corresponding to the sum

of their Hamming weights and a fixed width. The results show that the peak correlations of the single-island and two-island cases are close, and as the number of independent voltages increases, the correlation also increases. However, the correlation for a small number of independent voltages (between 2 and 8) remains well below that observed without dynamic voltage scaling.

5 ALIGNMENT ANALYSIS

iRDVS and DVS introduce temporal advantages for attack resistance in addition to improving SNR by amplitude scaling. According to the Sakurai-Newton delay model [6, 18], $\tau = \frac{C_L V}{k(V - V_T)^\alpha}$, the delay of the gates is closely related to the voltage supply. Assuming each independent voltage can change much faster than the duration of an attack, the power samples of the secret component will be shifted in time as the voltage changes. This means that the power samples associated with the secret operation, which were expected to be aligned, may be spread over a large range.

The work in [16] presents a relationship between misalignment and the correlation coefficient:

$$\rho(H, v^\alpha T) = \rho(H, v_s^\alpha T_s) * p * \sqrt{\frac{\text{Var}(v_s^\alpha T_s)}{\text{Var}(v^\alpha T)}} \quad (8)$$

where H represents the Hamming weight or Hamming distance matrix of the hypothetical intermediate value, $v^\alpha T$ denotes the power consumption at a certain time, $v_s^\alpha T_s$ refers to the portion of the power consumption caused by the secret operation, and p denotes the probability that the secret operation is consuming power at the attack time. Thus, $\rho(H, v_s^\alpha T_s)$ is the correlation for the case where the secret samples are perfectly aligned, whereas $\rho(H, v^\alpha T)$ is the correlation for the full design with misalignment. Having one or more dynamic voltages would lead to a small p by reducing the probability that secret power samples are self-aligned. iRDVS and DVS reduce p and decrease the correlation coefficient, making CPA attacks more difficult.

6 CLUSTERING ATTACK

Many alignment techniques, including elastic alignment [21], are based on a notion of a distance between traces. Power traces from similar operations can be aligned by minimizing the distance between them. Because voltage scaling increases the distance between operations, and multiple supplies add random noise, these techniques are ineffective when applied to our iRDVS approach, as we will show in Section 7. We propose to strengthen alignment attacks using a novel unsupervised ML-based algorithm that clusters the iRDVS traces into several groups that share similar voltage characteristics. After this clustering, we perform a CPA attack on every cluster and rank the possible subkeys based on their derived correlation coefficients, then average the rank of each possible subkey across all clusters and reorder the subkeys based on the average rank. This new rank order combines the information obtained from all individual attacks on all clusters. We pick the subkey with the lowest average rank to determine MTD, and determine PGE by the final rank of the correct subkey.

We propose using the computationally efficient K-means clustering algorithm [15] to group similar traces. This approach heuristically minimizes the distances among the power values of traces

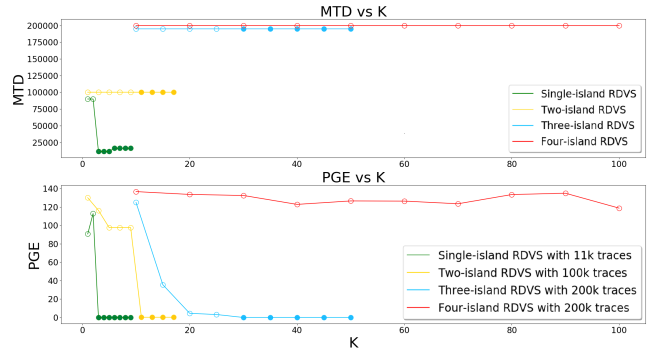


Figure 2: MTD and PGE iRDVS under clustering attack. Empty circles indicate unsuccessful attacks, whereas filled circles indicate successful attacks.

in each cluster. A critical parameter for K-means clustering is the number of clusters, which is generally set before the start of the clustering algorithm. We hypothesize that the number of clusters should match the number of different voltage combinations used in the trace set. In this way, each cluster will ideally contain traces from the same specific combination of voltages, ensuring the individual power samples containing the secret key are aligned.

Note that having many clusters implies that the average number of traces in each cluster will be K times smaller, reducing the effectiveness of the individual CPA analysis on each cluster. This motivates the experimental analysis, presented in the next section, of a range of K values to find the optimal number of clusters. Interesting future work includes using machine learning to guide the choice of K .

7 SIMULATION RESULTS AND ANALYSIS

This section describes how we evaluated the effectiveness of our iRDVS approach against alignment and CPA attacks.

7.1 Trace Generation and Experiment Design

We developed an in-house tool in Python to preprocess traces and perform CPA. Our tool converts power traces from various sources into a standard format, voltage scales the traces, and combines scaled traces to form synthetic iRDVS traces. It also performs CPA and clustering attacks on both the original and synthetic traces, and generates correlation coefficient, PGE, TVLA, and MTD metrics.

The original traces used for scaling and combining in these experiments are open-source traces from a combinational 128-bit AES implemented and measured on the Sasebo-GII board by Northeastern University [14]. We make each trace the power consumption of one voltage island. We use the Sakurai-Newton delay model [18] with $\alpha = 2$ to expand each sample in the original trace by interpolation, where V_{dd} for each island is randomly picked from the set $\{0.6, 0.7, 0.8, 0.9, 1\}$. We then add the scaled traces together to form the synthetic traces of our iRDVS design. This sum approximates a pipelined implementation of AES where each round operates simultaneously. To reduce the computation time and increase the probability of disclosure, we also extract the general region of interest from the synthetic traces before running CPA. Note that the original traces are a set of 100k, so to generate two island traces,

half of the traces are used as signal islands while the other half are used as noise islands, combined into a total of 50k traces. If we need more than 50k traces, we repeat this process with different scaling and combining of both the signal and noise traces. This means that the 50k signal plaintexts are repeated, but scaled differently and combined with different noise islands. For other multi-island traces, we applied similar methods to generate synthetic traces.

7.2 Effectiveness of Elastic Alignment

As described in Section 2, we tested preprocessing the traces using the open-source Python package *fastdtw* [19] to find the warp path, after which we applied elastic alignment based on Woudenberg et al.’s approach [21].

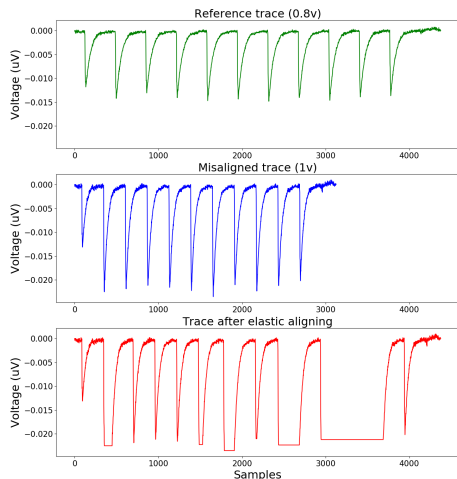


Figure 3: Example of elastic aligned trace after single-island DVS

However, even for the single-island DVS case, the elastic alignment does not perform nearly as well as for the frequency scaling case shown in Section 2. As illustrated in Figure 3, the aligned trace does not match up with the reference trace. The frequency differs from that of the reference trace, and there are gaps of no activity where none actually exists in the reference.

When we perform the same experiment with two independent voltages, the elastic technique is even less successful. The trace after alignment is almost the same as the original misaligned one, i.e., it yields negligible alignment that does not significantly help the attack. To further demonstrate the ineffectiveness of the elastic technique against iRDVS, we simplified iRDVS to two islands, fixed the voltage of the island to be attacked, and randomized the voltage of the other island, providing only two candidates for this random voltage. We first applied the elastic technique to these traces and then performed CPA on the elastic aligned traces. The results show that MTD remains larger than 100k traces and that the PGE increases from 49 to 148, suggesting that the elastic technique actually hurts the attack. Figure 3 shows how the elastic technique fails to align operations of interest even for $n = m = 1$, so for this $n = m = 2$ case we would expect that these operations would be further misaligned from one another, decreasing the attack success as we observed in Figure 2.

7.3 Resistance to Clustering

To analyze the potential benefits of clustering as a preprocessing step, we varied the number of clusters K and plotted MTD and PGE as functions of K . Figure 2 presents the MTD and PGE for $g = 5$ with the number of independent islands n ranging from one to four. 100k traces were used for $n = 1$ and 2, and 200k traces were used for $n = 3$ and 4, to account for the decreased cluster size described in Section 6. We assume that $m = n$ for every experiment.

For the single-island DVS case, using clustering reduces the MTD from over 100k ($K = 1$) down to 16k. This minimum is achieved when the number of clusters is well chosen ($K = 5$). For the two-island case, when the number of clusters is close to the ideal $K = 15$, the clustering attack can disclose most subkeys with 100k traces. Note that as illustrated in Figure 2, if the attackers are not able to correctly estimate K , the MTD exceeds 100k. For three-island iRDVS, for all values tested, the MTD was between 100k and 200k. The PGE reaches 0 when the number of clusters reaches the ideal $K = 35$, showing that the secret is disclosed when K is correctly specified. For the four-island case K was swept from 10 to 100, with the ideal being 70. The PGE at $K = 70$ is 123 and the MTD exceeds 200k, indicating that the secret is far from being uncovered.

8 MEASUREMENTS OF AN AES CHIP

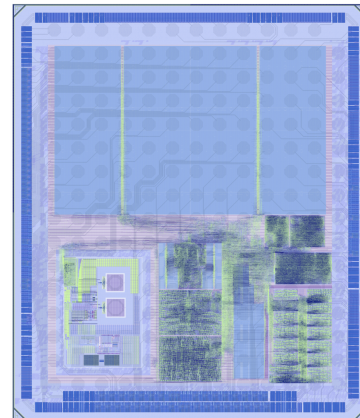


Figure 4: Die plot of the manufactured iRDVS chip

A chip was manufactured in a 12nm FinFet process to demonstrate the performance of the approach in silicon, Figure 4 presents its die plot. The chip included a 1GHz RISC-V complex for control and several variants of the AES core, both synchronous and asynchronous, including one with iRDVS protection. We found that with the AES cores running at 1GHz, it requires significant effort to identify precisely at what time the encryption batch starts and ends, and further effort to separate the encryption batch into individual encryptions. Previous analyses on simulated data expected separated encryption traces, so we modified the TVLA test to be able to perform the analysis without needing to separate encryption traces. The TVLA test was chosen because it does not require a successful or near-successful attack to obtain security results, and the non-specific test is attack-agnostic. Running one encryption at a time would not show the benefits of iRDVS, because iRDVS relies

on several islands operating at once for obfuscation, which requires several encryptions to be in different stages of the AES pipeline at once. While the traditional non-specific fixed-vs-random TVLA test compares the encryption of one fixed plaintext with the encryption of one “random” plaintext, we changed that one encryption to 32 encryptions, with the plaintext of interest (either fixed or random) in the middle of those 32 encryptions and the 31 other plaintexts being random. This ensures that the pipeline is as full as possible. The TVLA analysis was performed on the entire duration of those 32 encryptions. Each trace thus comprises a few thousand samples, with the number of samples varying proportionally with the time the core takes to complete the 32 operations (typically between 5K and 15K samples). To account for traces being different lengths due to natural variation and due to different voltage supply levels affecting the speed of encryption, the traces were linearly interpolated to all be of the same length. Traces are split into two groups of the same number of encryptions, and the t-test is run on both groups, each comprising half of the fixed and half of the random traces. The test then compares the fixed and random traces in each group. The TVLA methodology recommends a confidence value C of 4.5, which means that any samples with t-scores < -4.5 or > 4.5 in both groups indicate that the device is insecure and “fails” with a confidence of 99.99%. To further demonstrate the strength of the iRDVS approach, the same analysis was performed for a C value of 2 and the results are summarized in Table 1.

In particular, our TVLA analysis compared four cases: constant voltage, DVS, adjacent iRDVS, and alternating iRDVS, all running on the iRDVS AES core. The constant voltage case runs all encryptions at a constant of 0.8V. The DVS case keeps all islands at the same voltage but changes that voltage randomly to a value between 0.6V and 0.8V for every encryption batch. The adjacent and alternating iRDVS configurations use the full capability of the iRDVS core and change the voltage of each of the four power domains randomly and independently for every encryption batch. These adjacent and alternating cases extend the same cases from the simulation experiments to use four independent voltage domains rather than two. We predict that stages with similar delay maximize overlapping computation and minimize potential timing side channels. For this reason, every other flip-flop is transparent, creating seven pipeline stages, each with two rounds of AES and two voltage islands.

Table 1: Non-specific fixed-vs.-random TVLA results - # of samples with t-scores exceeding C

Case	$C = 4.5$	$C = 2.0$
Constant	740	2211
DVS	0	34
Adjacent iRDVS	0	12
Alternating iRDVS	0	4

9 CONCLUSIONS AND FUTURE WORK

According to mathematical analysis and experimental results, the proposed island-based random DVS approach not only maintains the merits of DVS but also introduces misalignment that is resistant to advanced alignment techniques. The proposed unsupervised machine learning based attack is successful with three or fewer islands but increases in difficulty as the number of islands grows.

This is in part because the number of voltage supply settings grows combinatorially with the number of independent voltages.

An AES iRDVS chip was fabricated to demonstrate the security benefits of the approach, using the industry-accepted TVLA methodology and resulting metric. Further work can be done with larger sample sizes, and work can be done to separate encryption traces precisely so that individual encryptions can be analyzed with TVLA and attacked with CPA or other power analysis attacks. The DVS and adjacent and alternating island-based RDVS cases comprise only a small portion of the potential design space for the iRDVS AES core. Our future work includes finding the most secure configuration as well as finding the configurations that best balances security, performance, and power. Future efforts will also include the addition of voltage generation and randomization circuitry as part of the core. This will further improve the security of the system by reducing the attack surface of the core.

10 ACKNOWLEDGEMENT

This work, including the fabrication of the chip presented, was supported by DARPA under the “21 Century Cryptography” program and contract #HR001119C0070.

REFERENCES

- [1] K. Baddam and M. Zvolinski. 2007. Evaluation of Dynamic Voltage and Frequency Scaling as a Differential Power Analysis Countermeasure. In *VLSI*. 854–862.
- [2] A. G. Bayrak, N. Velickovic, F. Regazzoni, D. Novo, P. Brisk, and P. Jenne. 2013. An EDA-friendly Protection Scheme against Side-Channel Attacks. In *2013 DATE*.
- [3] Georg T. Becker, Jim Cooper, Elizabeth K. DeMulder, Gilbert Goodwill, Joshua Jaffe, Gary Kenworthy, T. Kouzminov, Andrew J. Leiserson, Mark E. Marson, Pankaj Rohatgi, and Sami Saab. 2013. Test Vector Leakage Assessment (TVLA) methodology in practice. In *2013 ICMC*.
- [4] P. A. Beerel, R. O. Ozdag, and M. Ferretti. 2010. *A Designer’s Guide to Asynchronous VLSI*. Cambridge University Press.
- [5] Eric Brier, Christophe Clavier, and Francis Olivier. 2004. Correlation Power Analysis with a Leakage Model. In *2004 CHES*. 16–29.
- [6] A. P. Chandrakasan, S. Sheng, and R. W. Brodersen. 1992. Low-power CMOS Digital Design. *IEEE JSSC* 27, 4 (1992), 473–484.
- [7] Dake Chen, Xuan Zhou, Yinghua Hu, Yuke Zhang, Kaixin Yang, Andrew Rittenbach, Pierluigi Nuzzo, and Peter A. Beerel. 2023. Unraveling Latch Locking Using Machine Learning, Boolean Analysis, and ILP. In *2023 24th International Symposium on Quality Electronic Design (ISQED)*. 1–8. <https://doi.org/10.1109/ISQED57927.2023.10129346>
- [8] Alexander DeTrano, Sylvain Guillely, Xiaofei Guo, Naghme Karimi, and Ramesh Karri. 2015. Exploiting Small Leaks in Masks to Turn a Second-order Attack into a First-order Attack. In *2015 HASP*. 7:1–7:5.
- [9] Darshana Jayasinghe, Aleksandar Ignjatovic, and Sri Parameswaran. 2019. SCRIIP: Secure Random Clock Execution on Soft Processor Systems to Mitigate Power-based Side Channel Attacks. In *2019 IEEE/ACM ICCAD*. IEEE, 1–7.
- [10] M. Kar, A. Singh, S. Mathew, A. Rajan, V. De, and S. Mukhopadhyay. 2017. Invited paper: Low power requirements and side-channel protection of encryption engines: Challenges and opportunities. In *IEEE/ACM ISLPED*. 1–2.
- [11] Paul Kocher, Joshua Jaffe, and Benjamin Jun. 1999. Differential Power Analysis. In *Annual International Cryptology Conference*. 388–397.
- [12] P. Liu, H. Chang, and C. Lee. 2012. A True Random-Based Differential Power Analysis Countermeasure Circuit for an AES Engine. *IEEE Trans. Circuits Syst. II: Express Br.* 59, 2 (2012), 103–107.
- [13] Yingxi Lu, Maire P. O’Neill, and John V. McCanny. 2008. FPGA Implementation and Analysis of Random Delay Insertion Countermeasure against DPA. In *2008 ICFT*. 201–208.
- [14] P. Luo, Y. Fei, L. Zhang, and A. A. Ding. 2014. Side-channel Power Analysis of Different Protection Schemes against Fault Attacks on AES. In *2014 ReConFig*.
- [15] James MacQueen et al. 1967. Some Methods for Classification and Analysis of Multivariate Observations. In *Proc. of the Fifth Berkeley Symposium on Mathematical Statistics and Probability*, Vol. 1. 281–297.
- [16] Stefan Mangard. 2004. Hardware Countermeasures against DPA—a Statistical Analysis of Their Effectiveness. In *Cryptographers’ Track at the RSA*. 222–235.
- [17] C. O’Flynn and Z. David Chen. 2015. Side channel power analysis of an AES-256 bootloader. In *2015 IEEE CCECE*. 750–755.

- [18] T. Sakurai and A. R. Newton. 1990. Alpha-power Law MOSFET Model and Its Applications to CMOS Inverter Delay and Other Formulas. *IEEE JSSC* 25, 2 (1990), 584–594.
- [19] Stan Salvador and Philip Chan. 2007. Toward Accurate Dynamic Time Warping in Linear Time and Space. *Intelligent Data Analysis* 11, 5 (2007), 561–580.
- [20] A. Singh, M. Kar, S. Mathew, A. Rajan, V. De, and S. Mukhopadhyay. 2017. Improved Power Side Channel Attack Resistance of a 128-bit AES Engine with Random Fast Voltage Dithering. In *IEEE ESSCIRC*. 51–54.
- [21] Jasper G. J. van Woudenberg, Marc F. Witteman, and Bram Bakker. 2011. Improving Differential Power Analysis by Elastic Alignment. In *Topics in Cryptology - CT-RSA 2011 (LNCS)*. 104–119.
- [22] Shengqi Yang, W. Wolf, N. Vijaykrishnan, D.N. Serpanos, and Yuan Xie. 2005. Power attack resistant cryptosystem design: a dynamic voltage and frequency switching approach. In *2005 DATE*. 64–69 Vol. 3.
- [23] W. Yu and S. Köse. 2017. False Key-Controlled Aggressive Voltage Scaling: A Countermeasure Against LPA Attacks. *IEEE TCAD* 36, 12 (2017), 2149–2153.
- [24] W. Yu and S. Köse. 2018. Exploiting Voltage Regulators to Enhance Various Power Attack Countermeasures. *IEEE Trans. Emerg. Top. Comput.* 6, 2 (2018), 244–257.